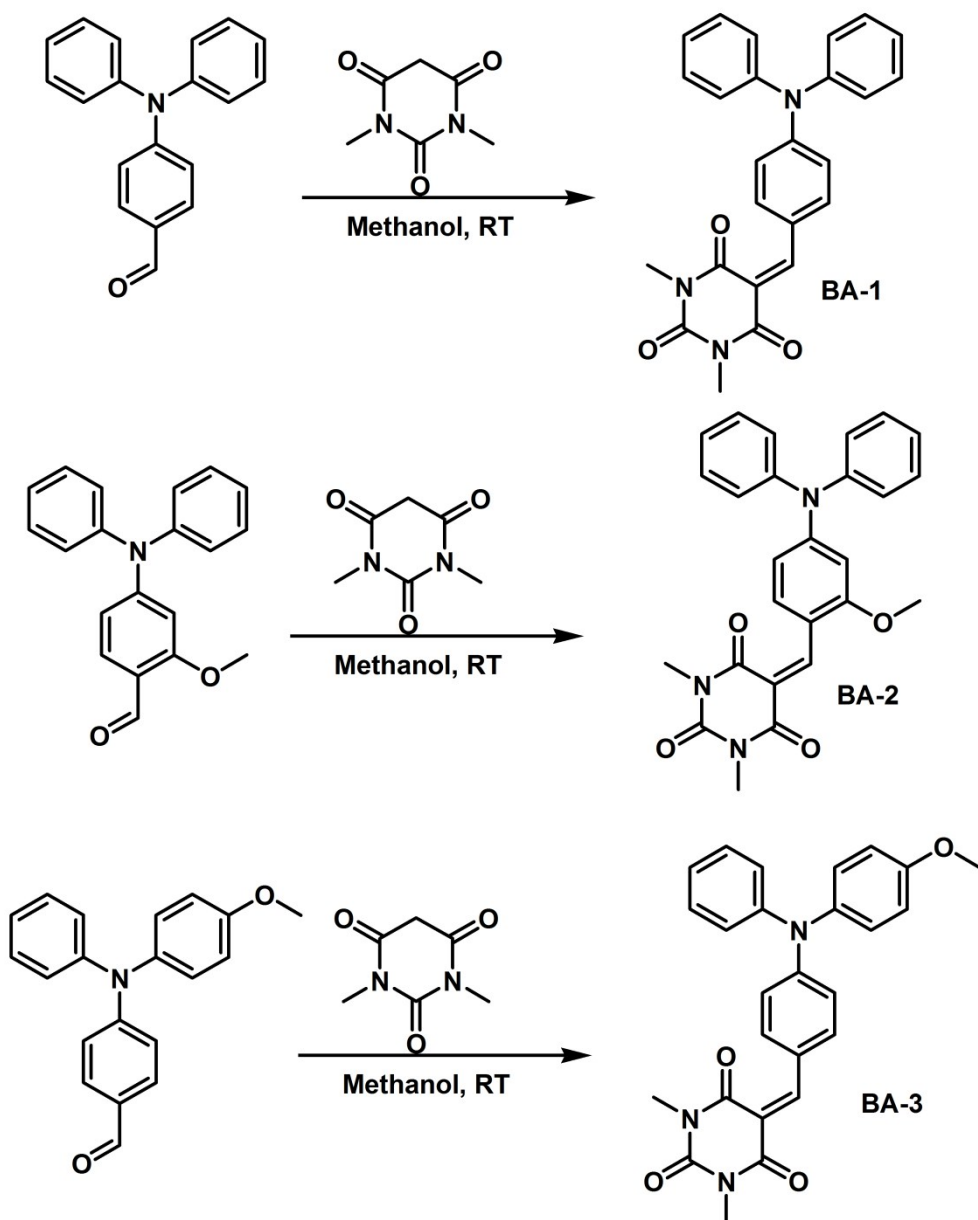


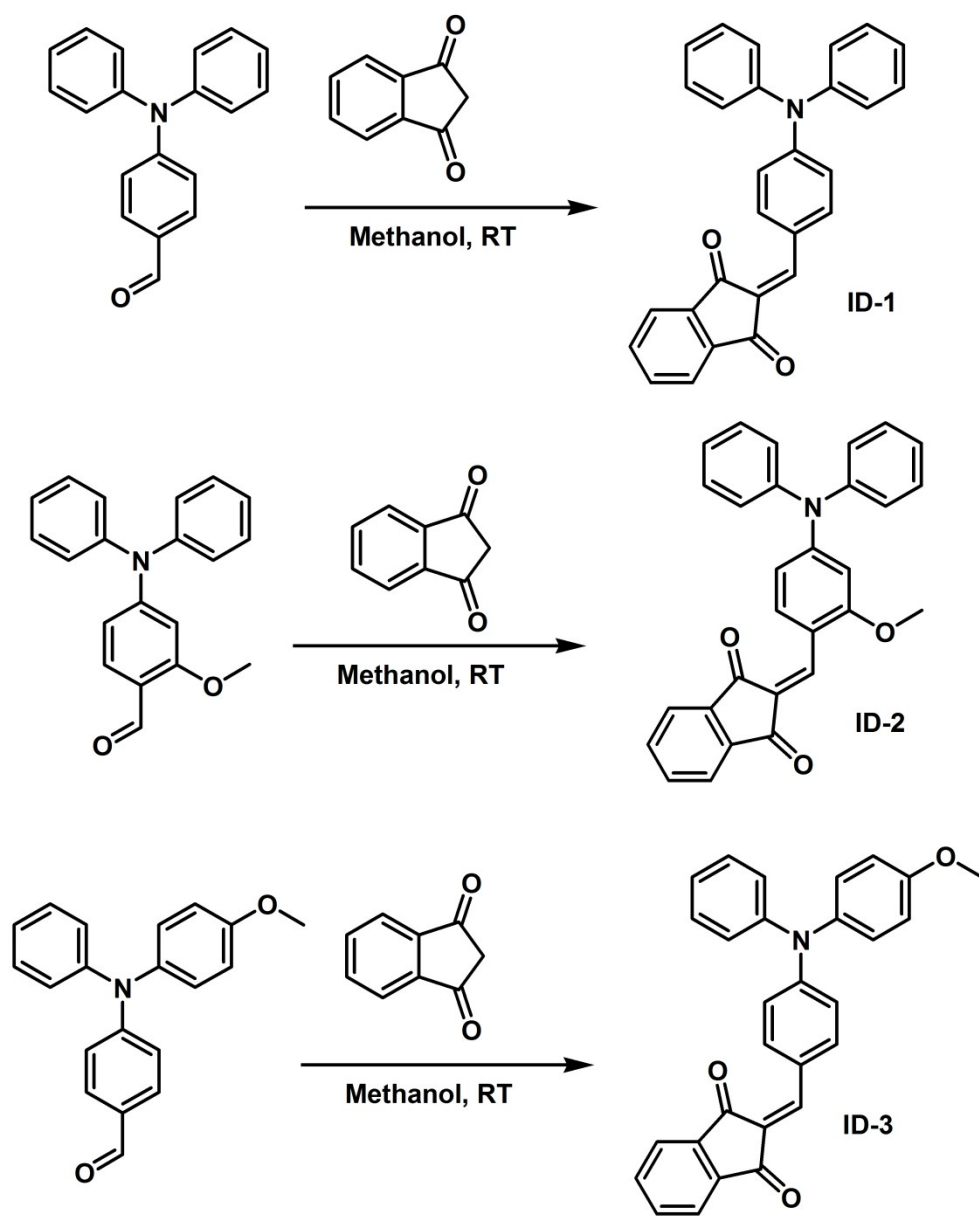
Supporting Information

**Synthesis of tunable, red fluorescent aggregation enhanced emissive organic fluorophores:
Stimuli responsive high contrast off-on fluorescence switching**

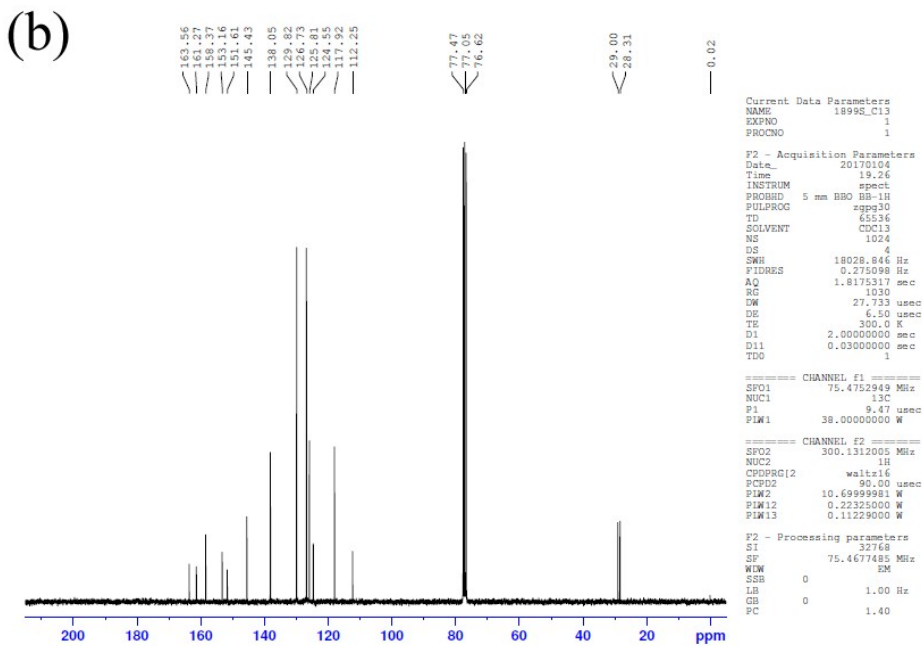
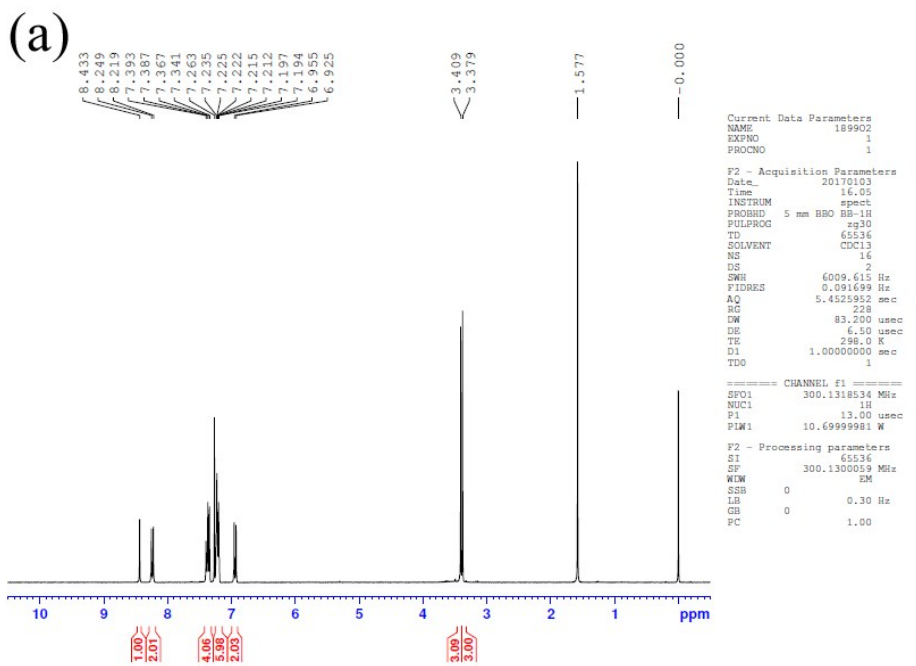
Palamarneri Sivaraman Hariharan, Parthasarathy Gayathri, Anu Kundu, Subramanian
Karthikeyan, Dohyun Moon and Savarimuthu Philip Anthony*



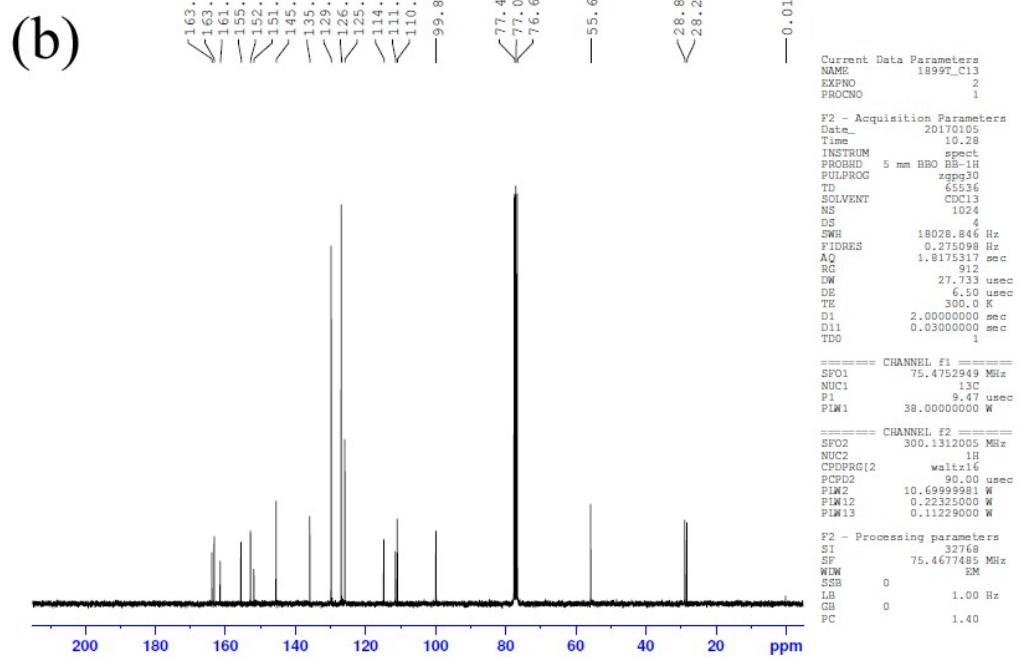
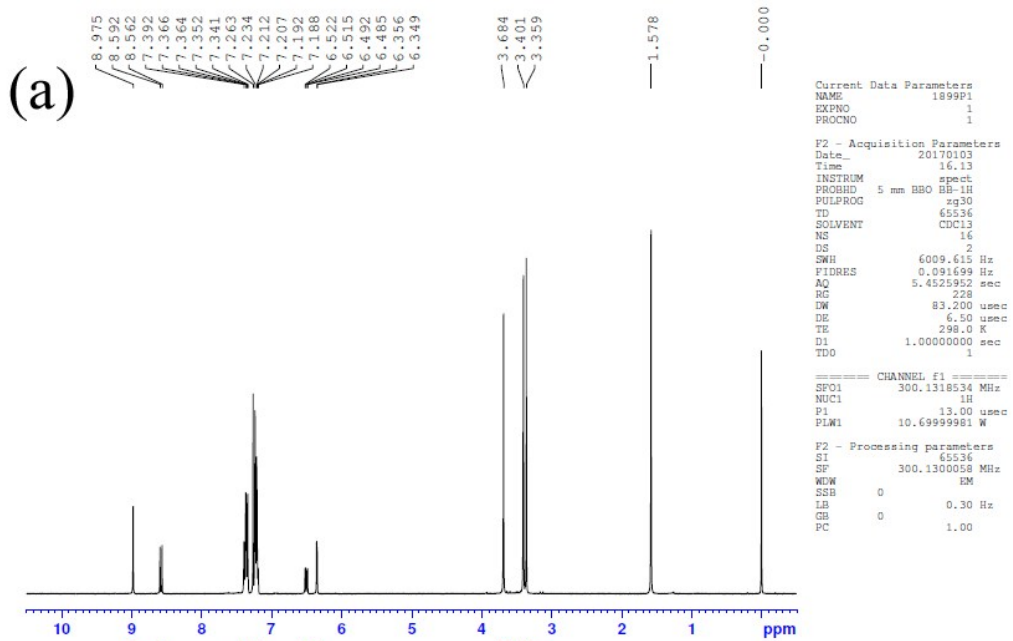
Scheme S1. Synthesis of BA compounds.



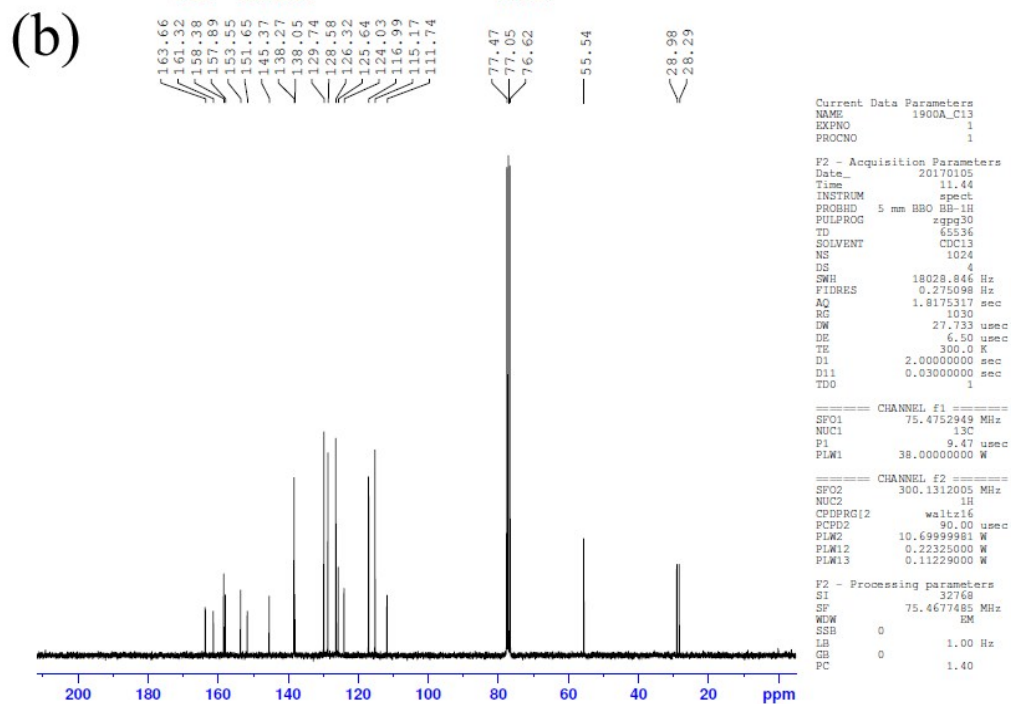
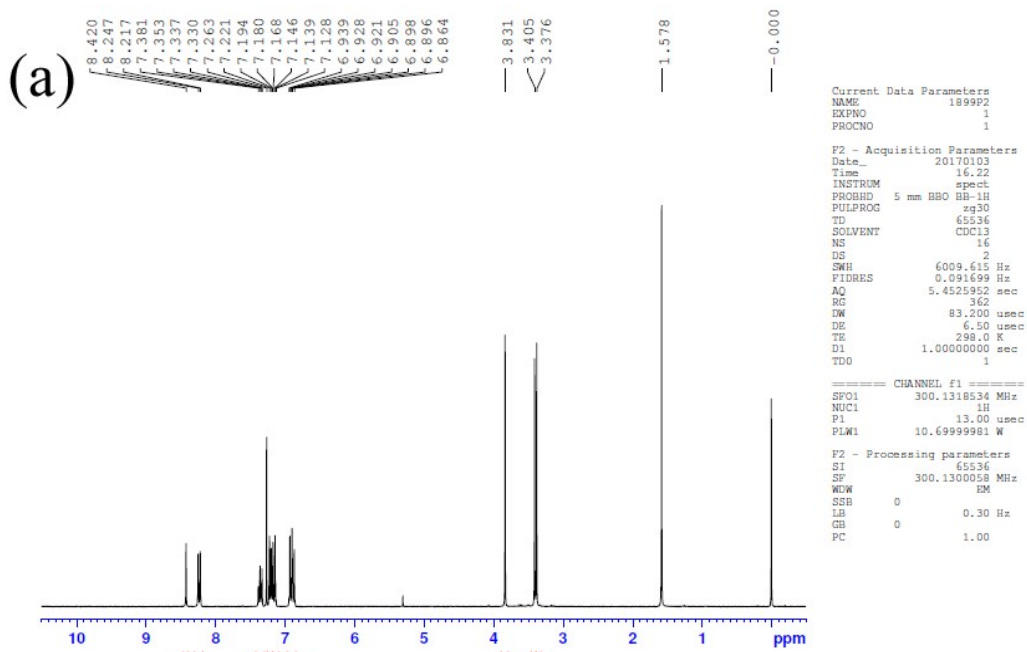
Scheme S2. Synthesis of ID compounds.



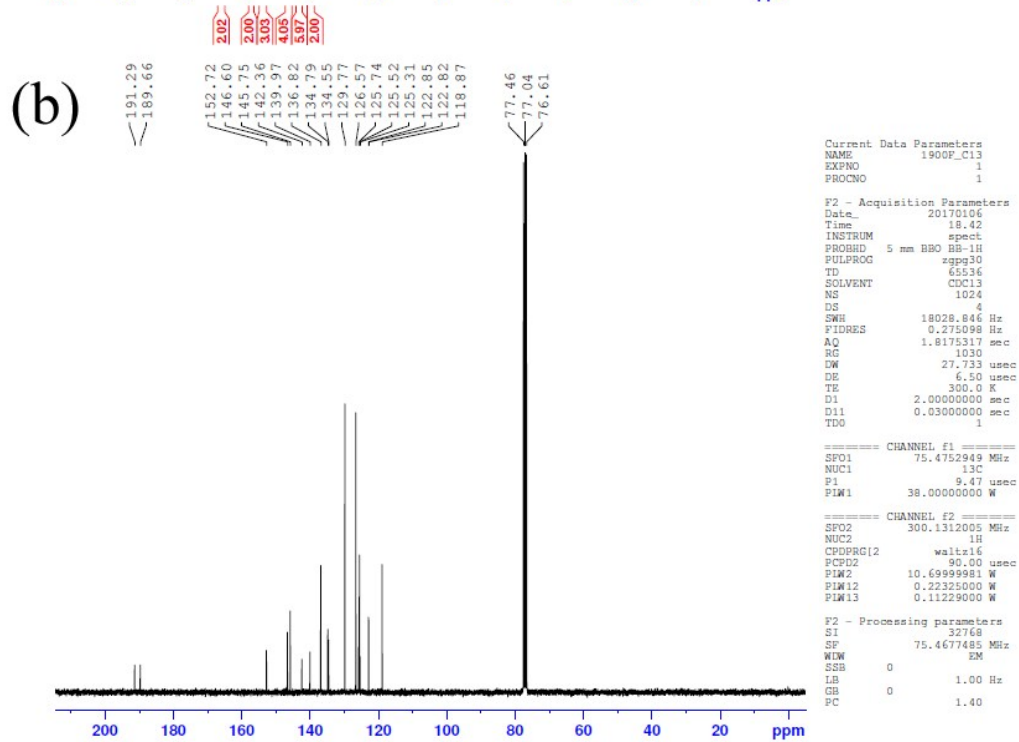
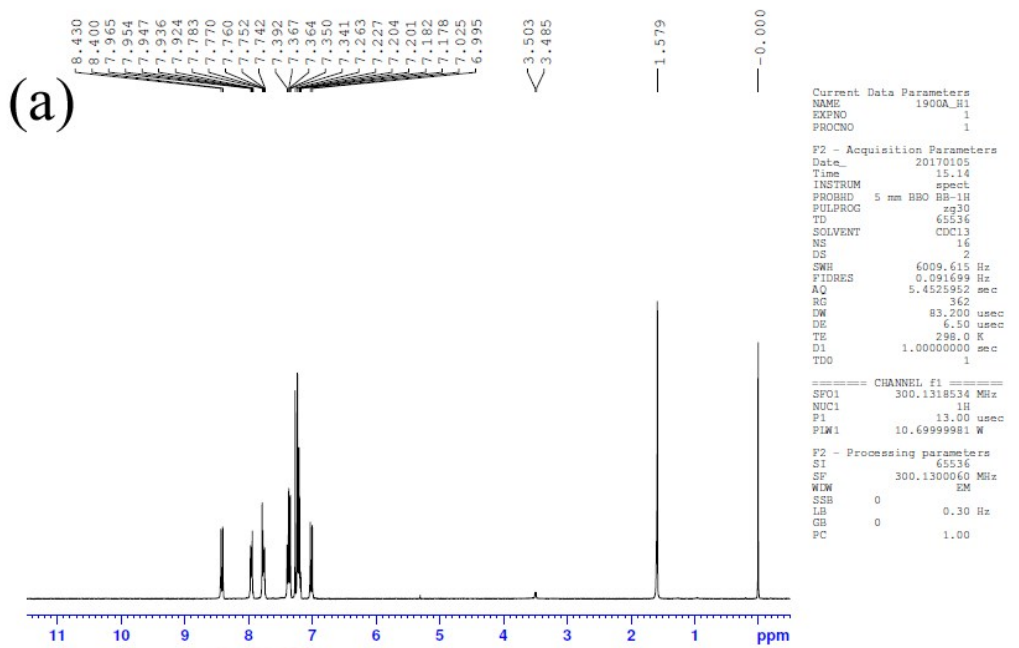
(a) ^1H and (b) ^{13}C -NMR spectra of BA-1.



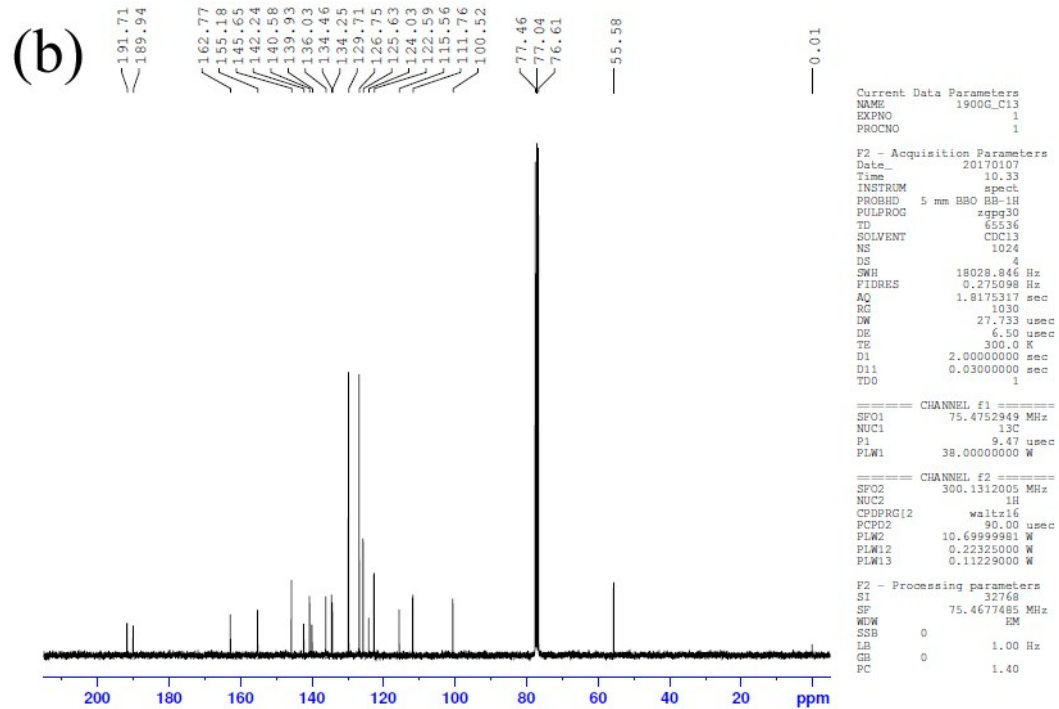
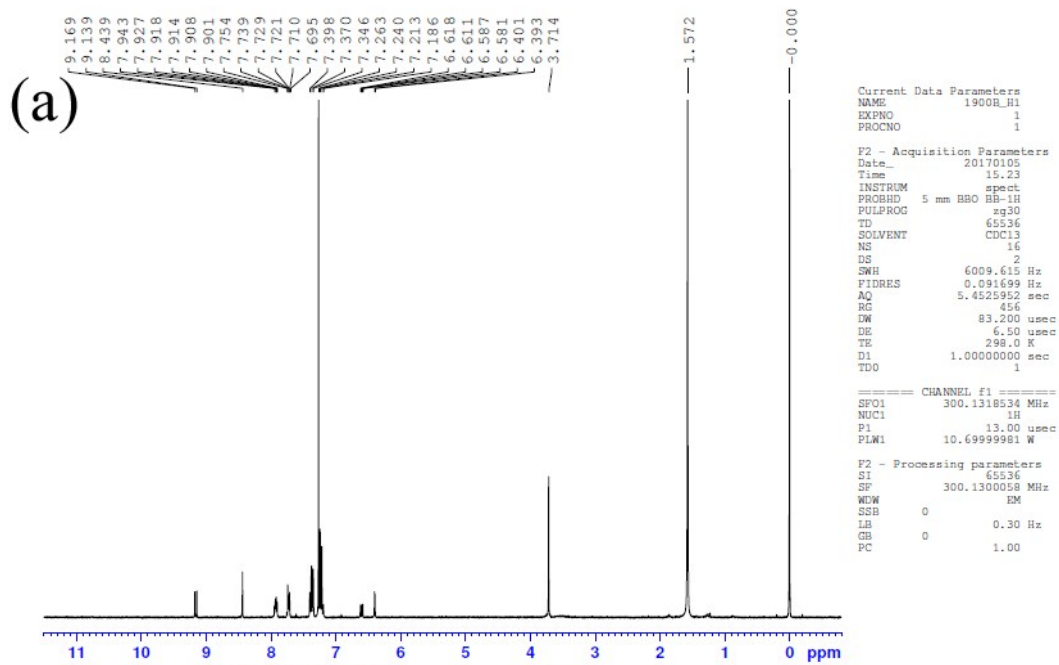
(a) ^1H and (b) ^{13}C -NMR spectra of BA-2.



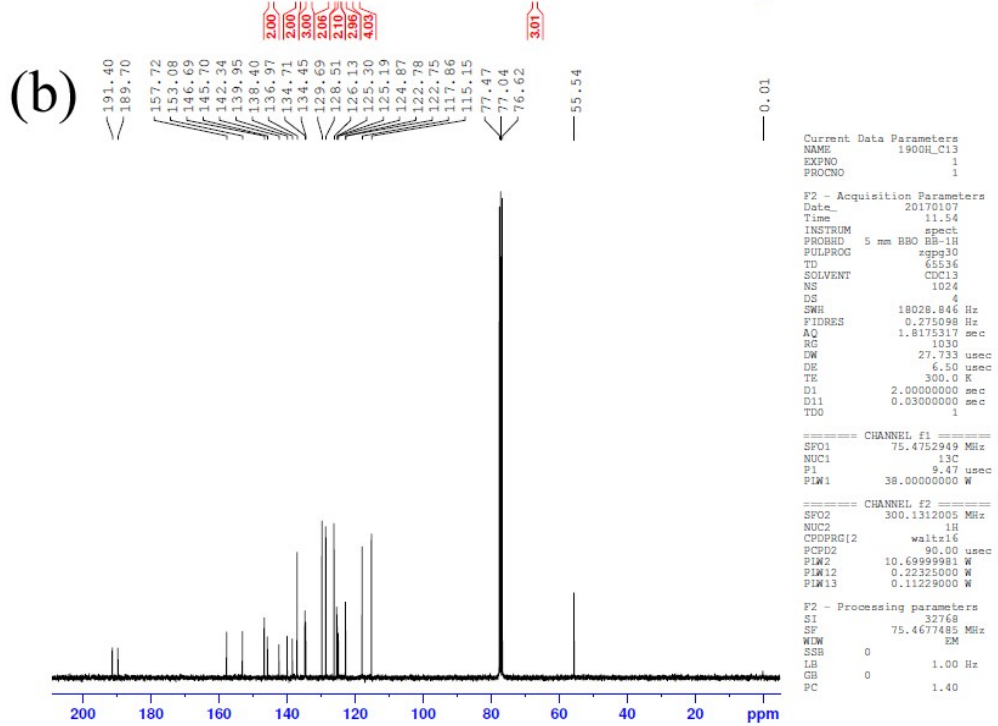
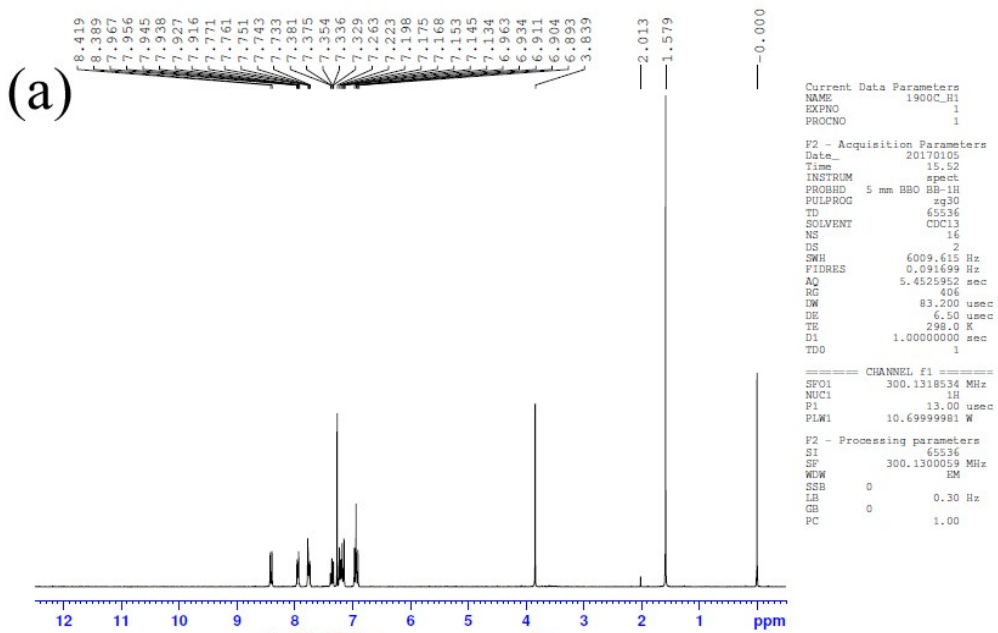
(a) ^1H and (b) ^{13}C -NMR spectra of BA-3.



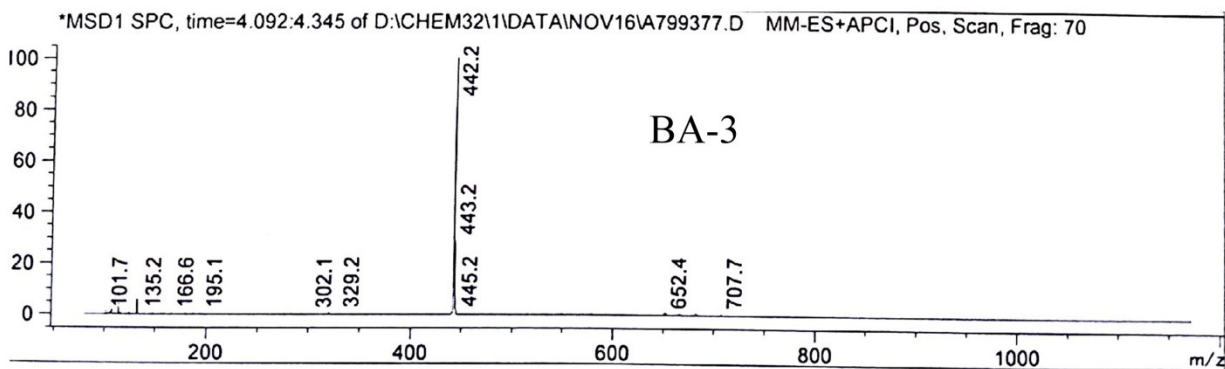
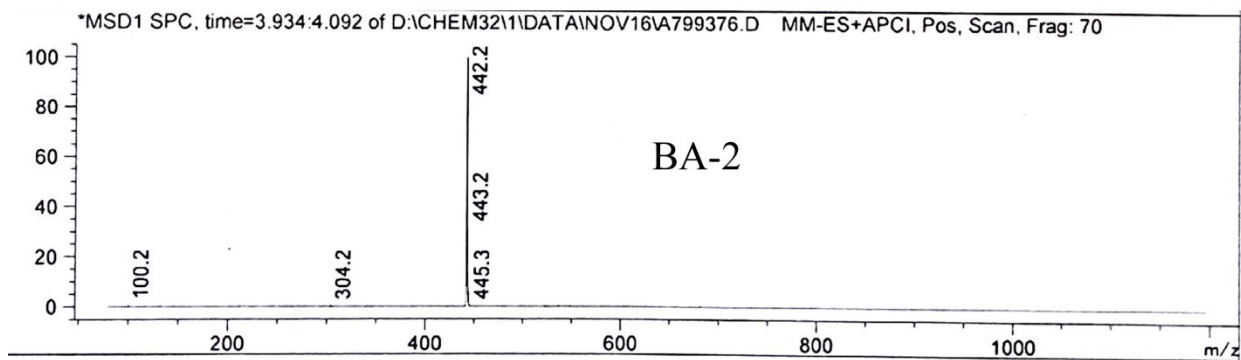
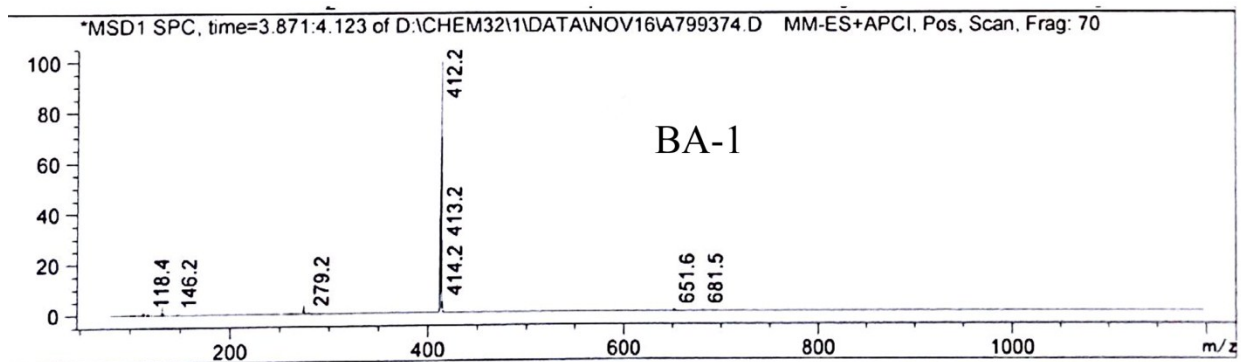
(a) ^1H and (b) ^{13}C -NMR spectra of ID-1.



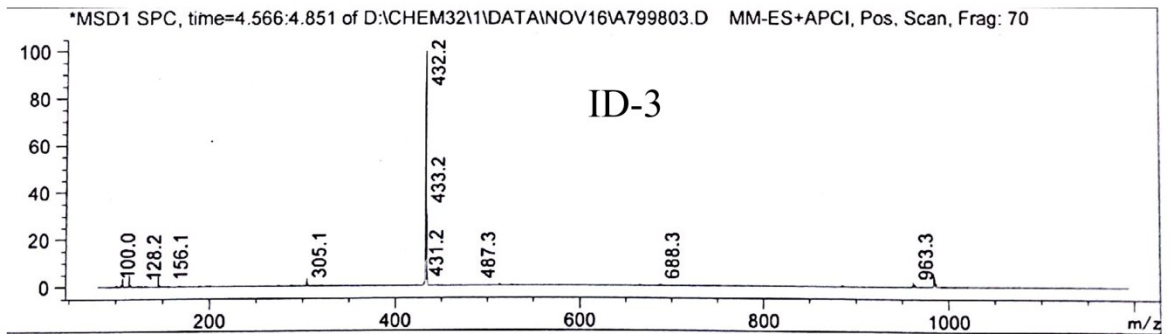
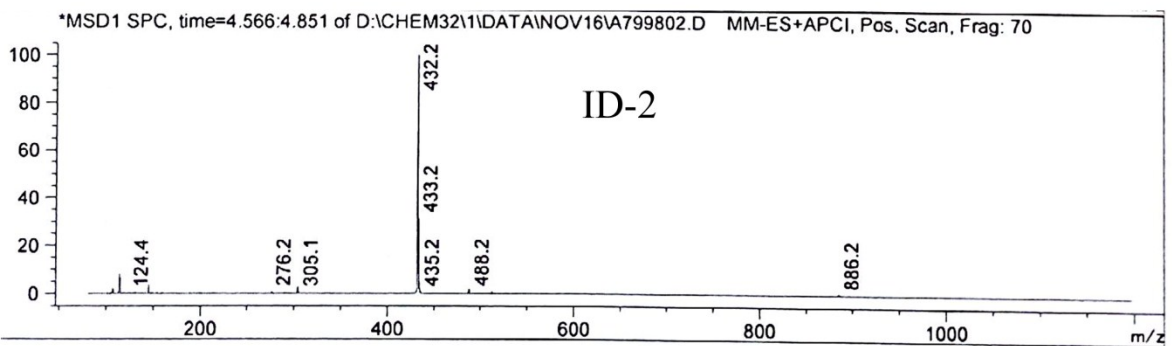
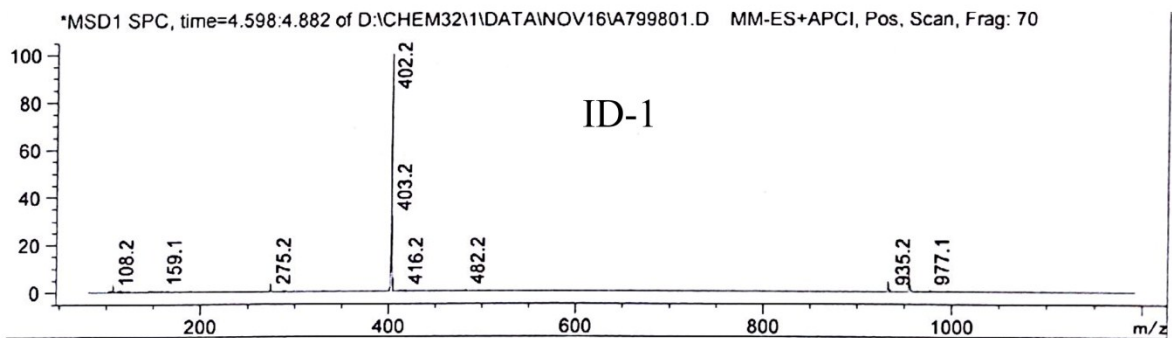
(a) ^1H and (b) ^{13}C -NMR spectra of ID-2.



(a) ^1H and (b) ^{13}C -NMR spectra of ID-3.



Mass spectra of BA compounds.



Mass spectra of ID compounds.

Table S1. Quantum yields of BA and ID compounds in CH₃CN and CH₃CN-water mixture.

Solvents	BA-1 (Φ_f)	BA-2 (Φ_f)	BA-3 (Φ_f)	ID-1 (Φ_f)	ID-2 (Φ_f)	ID-3 (Φ_f)
CH ₃ CN	0.0008	0.0026	0.0012	0.00098	0.0016	0.0019
CH ₃ CN- Water	0.0231	0.080	0.032	0.0067	0.01	0.012

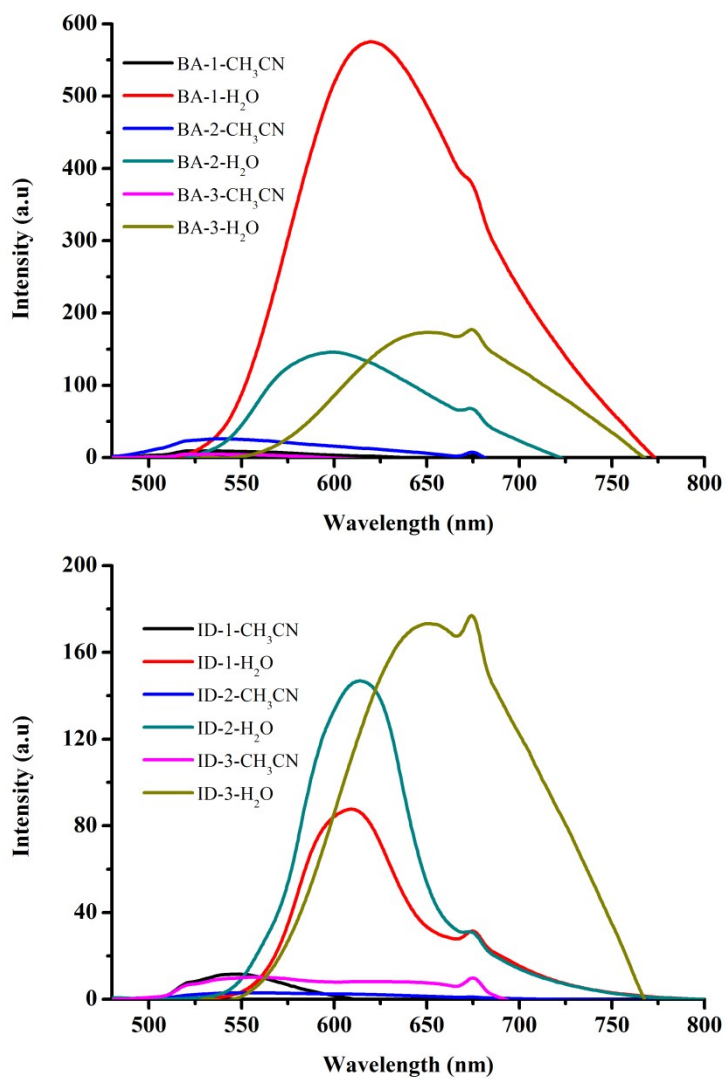


Fig. S1. Fluorescence spectra of BA and ID compounds in CH₃CN and CH₃CN-water mixture.

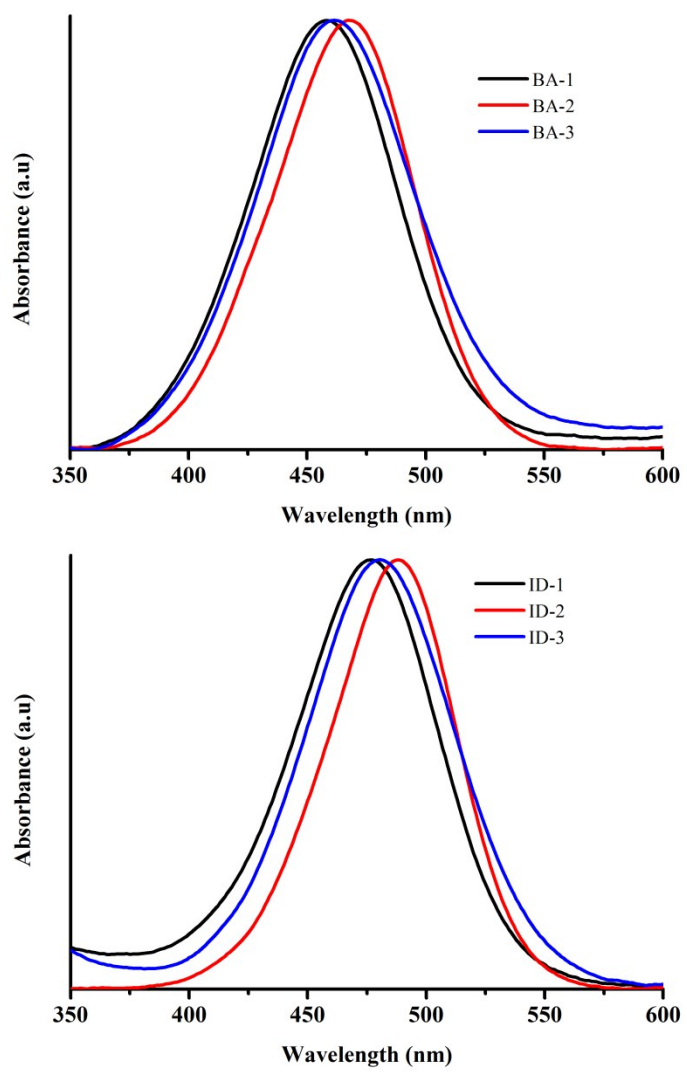


Fig. S2. Absorption spectra of BA and ID compounds in CH_3CN .

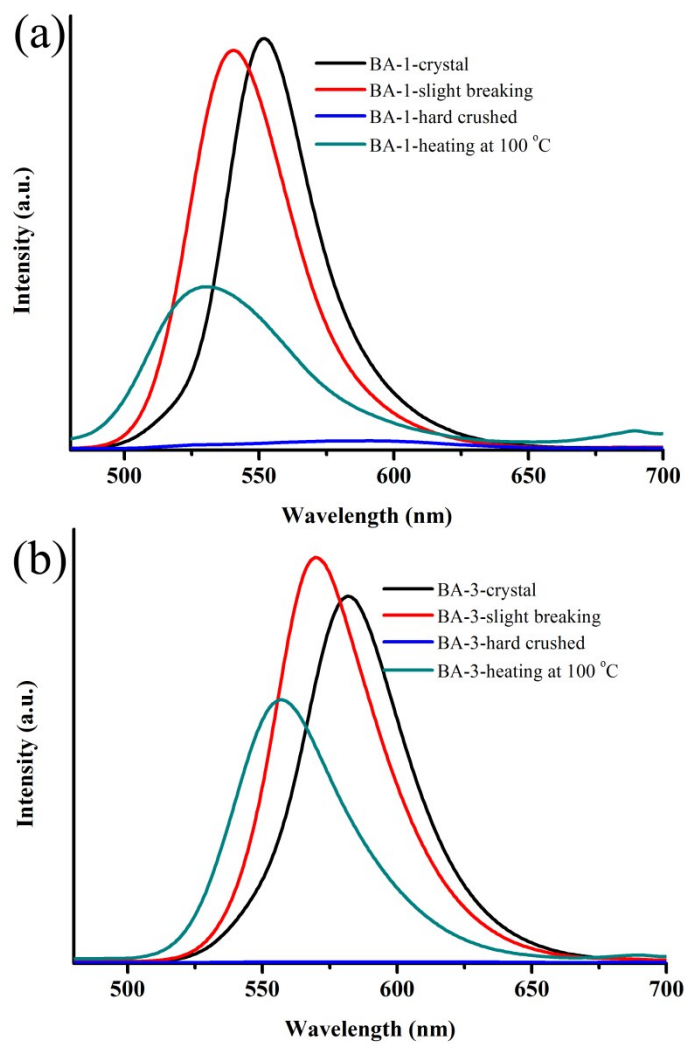


Fig. S3. Solid state fluorescence switching of (a) BA-1 and (b) BA-3 by external stimuli. ($\lambda_{\text{exc}} = 370$ nm).

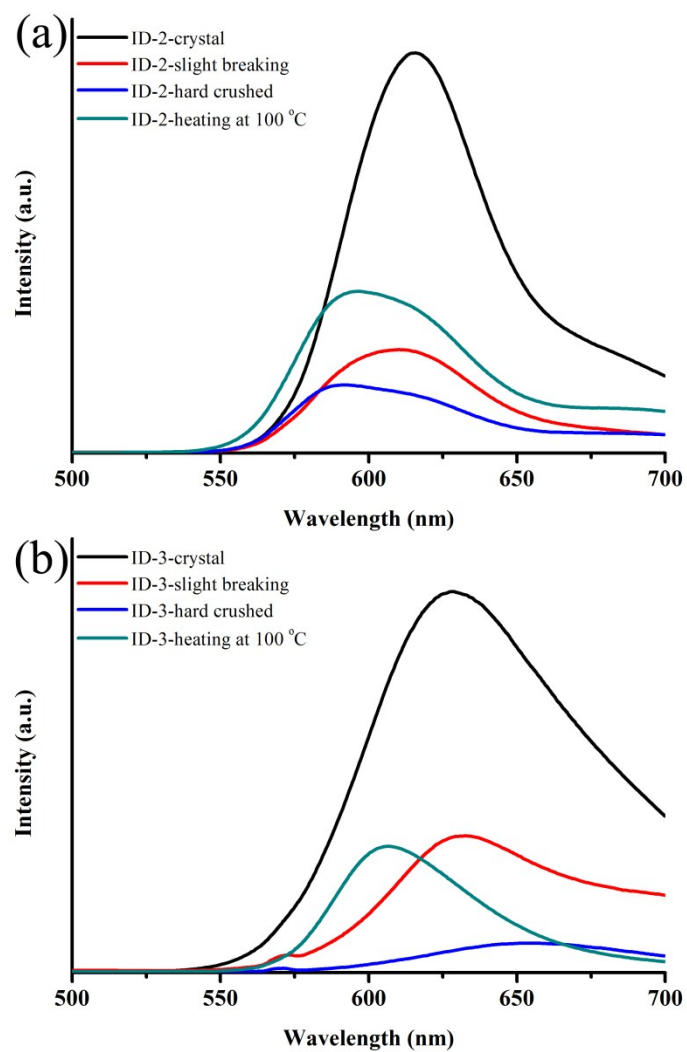


Fig. S4. Solid state fluorescence switching of (a) ID-2 and (b) ID-3 by external stimuli. ($\lambda_{\text{exc}} = 370 \text{ nm}$).

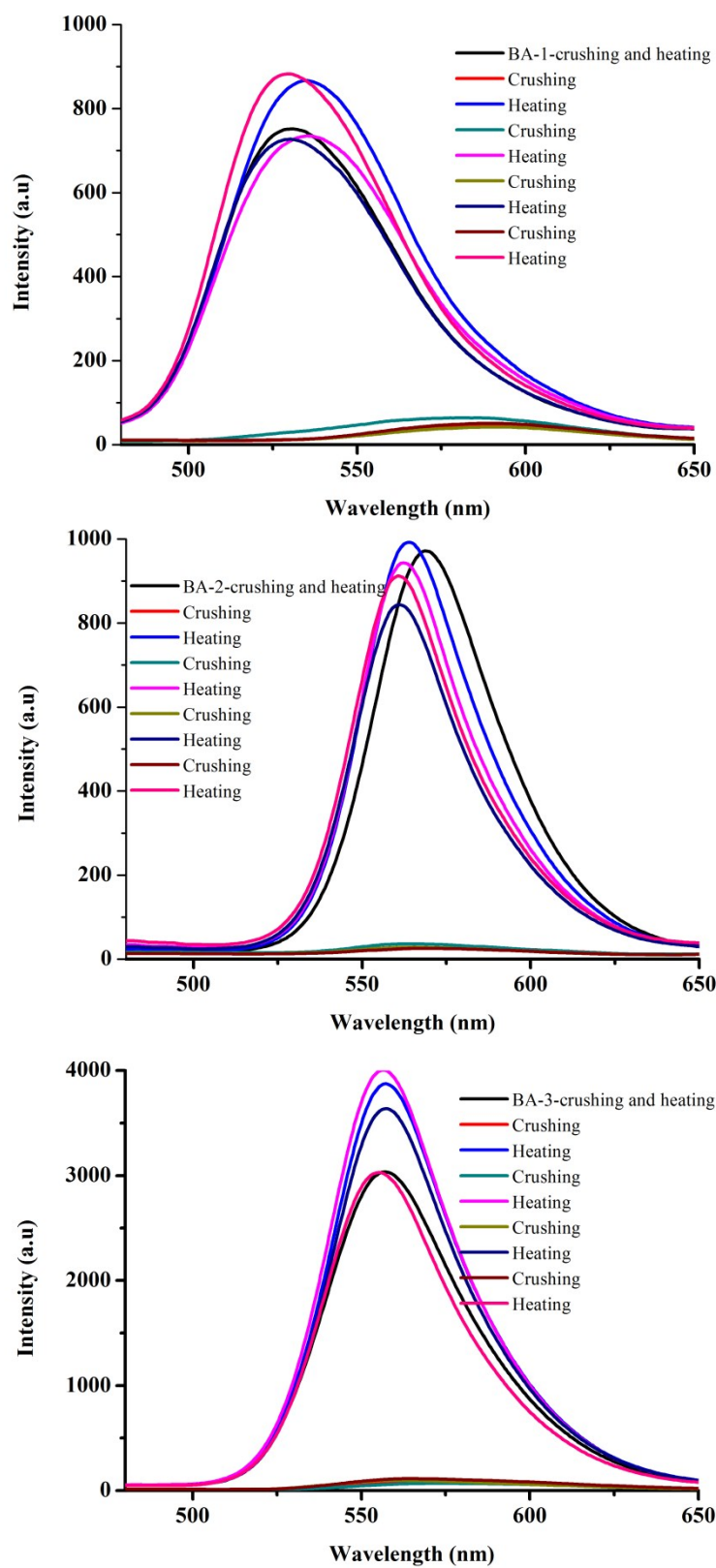


Fig. S5. Solid state fluorescence switching of BA-1-3 by strong crushing followed by heating. ($\lambda_{exc} = 370$ nm).

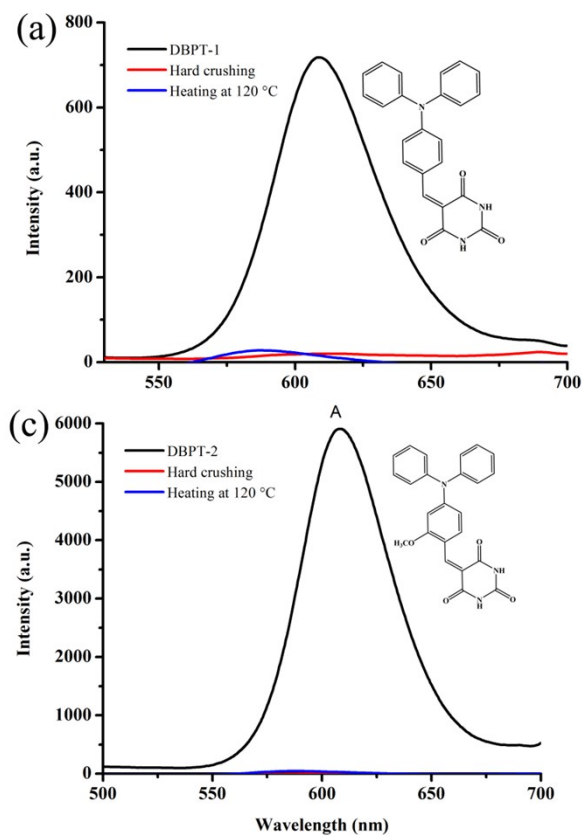


Fig. S6. Solid state fluorescence spectra of (a) DPBT-1 and (b) DPBT-2. ($\lambda_{\text{exc}} = 370 \text{ nm}$).

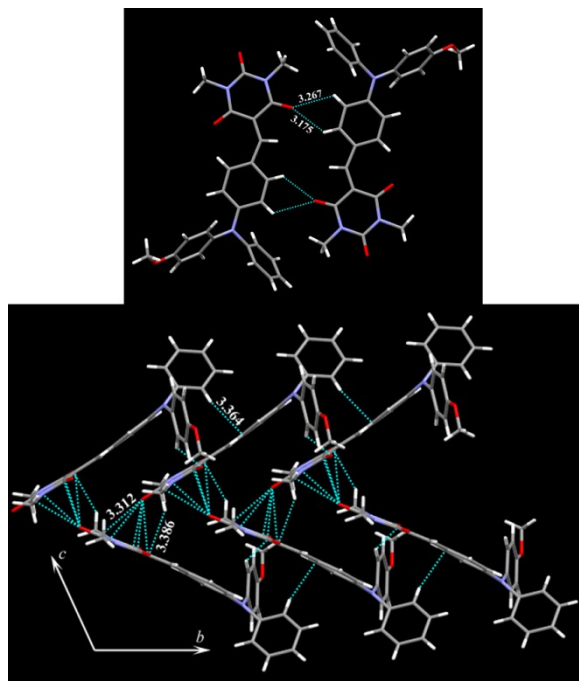


Fig. S7. Dimer formation via H-bonding interaction between oxygen of N-methyl barbituric acid and phenyl hydrogen and extended H-bonding interaction in the crystal lattice of BA-3. C (grey), N (blue), O (red), H (white). H-bonding interactions (broken line) distances are marked in Å.

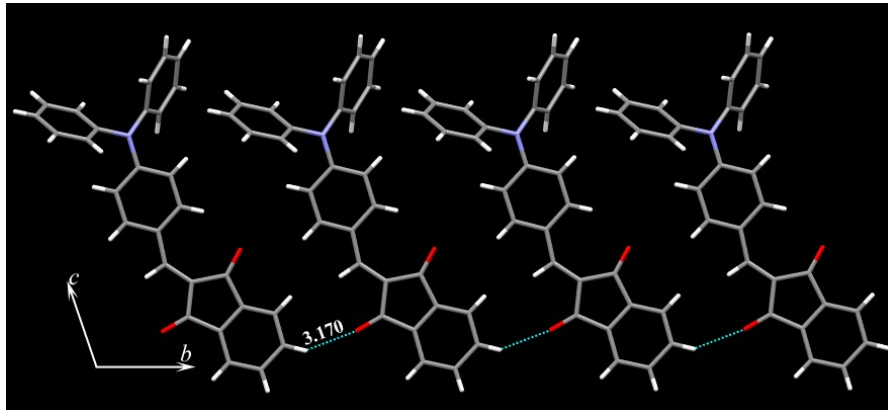


Fig. S8. H-bonding interaction between oxygen of indane dione and indane dione phenyl hydrogen in the crystal lattice of ID-1. C (grey), N (blue), O (red), H (white). H-bonding interactions (broken line) distances are marked in Å.

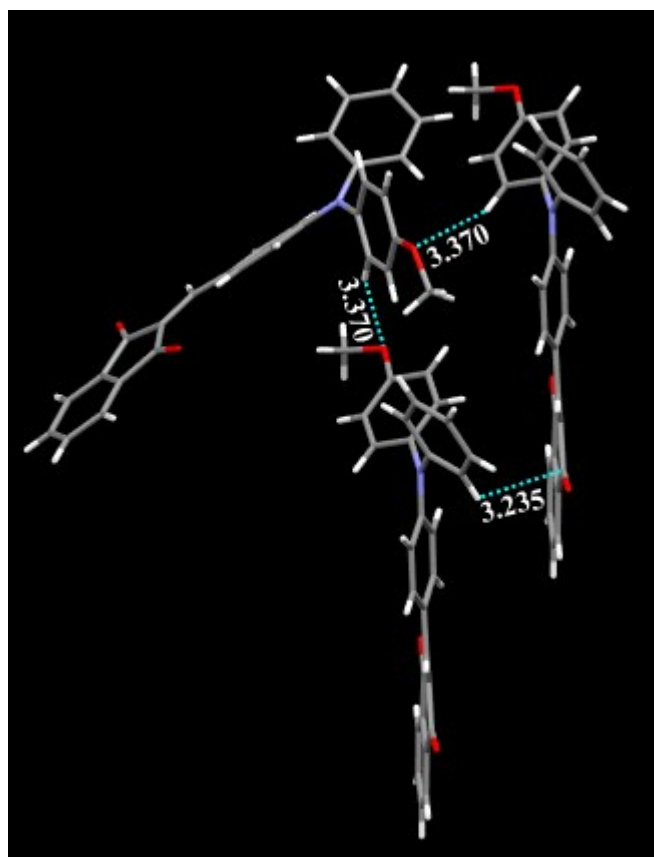


Fig. S9. H-bonding interactions in the crystal lattice of ID-3. C (grey), N (blue), O (red), H (white). H-bonding interactions (broken line) distances are marked in Å.

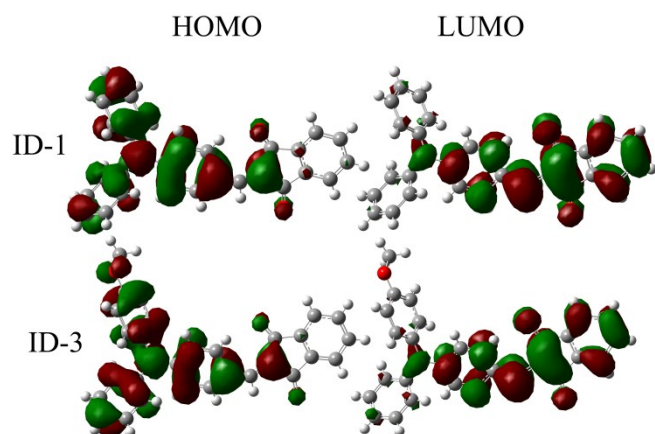


Fig. S10. Molecular orbital plots of the HOMOs and LUMOs of ID compounds.

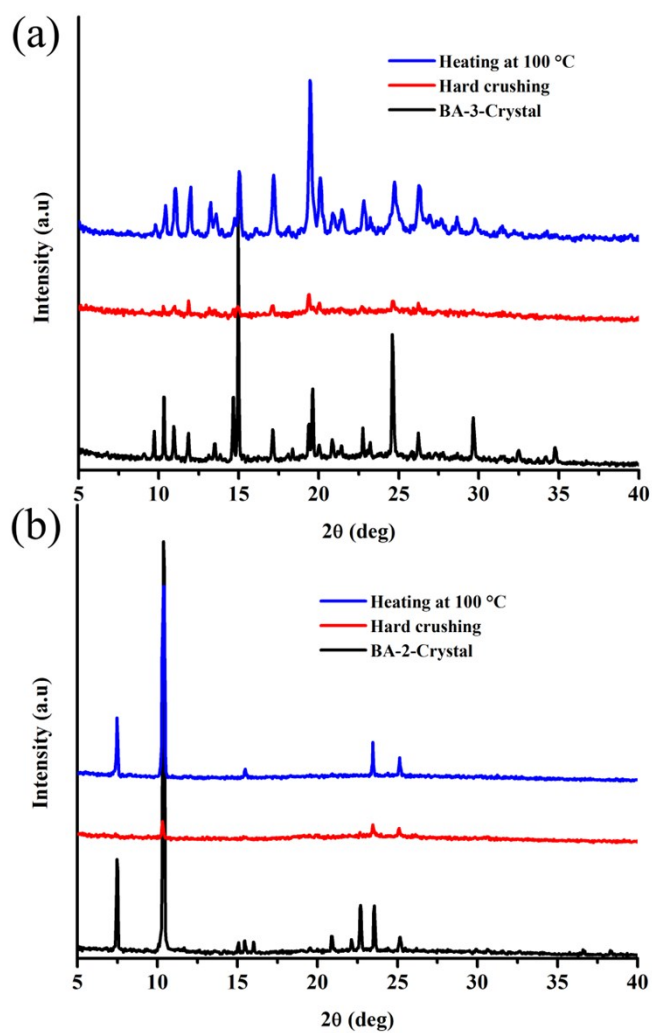


Fig. S11. PXRD pattern of (a) BA-2 and (b) BA-3 before, after hard crushing and heating.

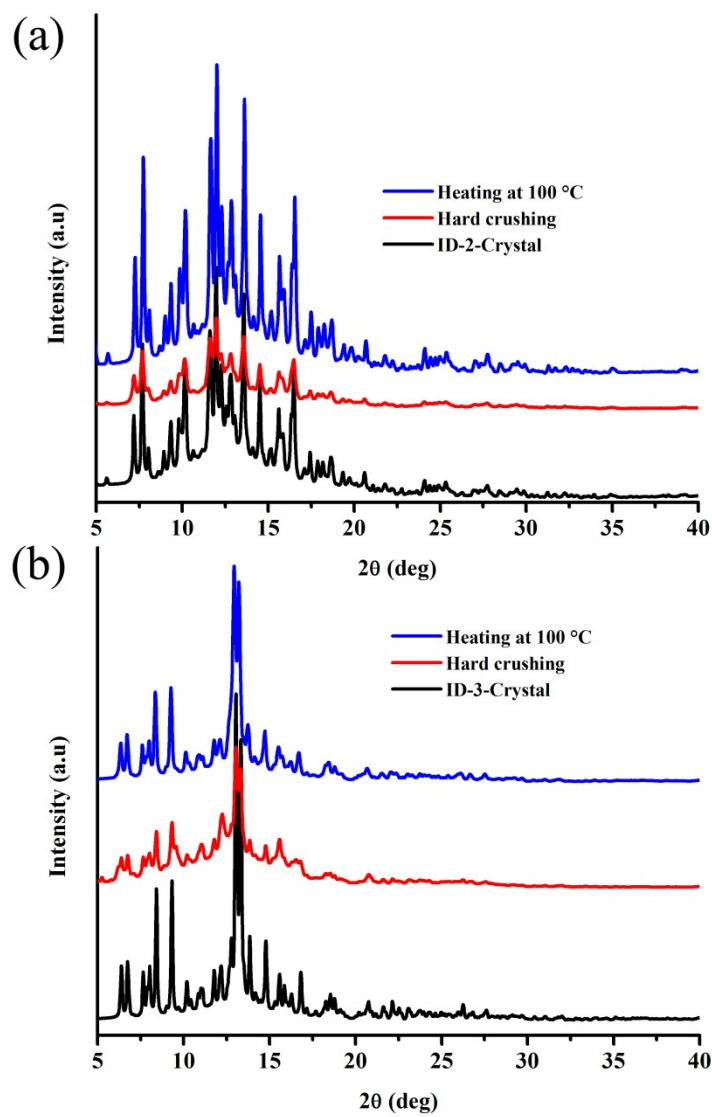


Fig. S12. PXRD pattern of (a) ID-2 and (b) ID-3 before, after hard crushing and heating.

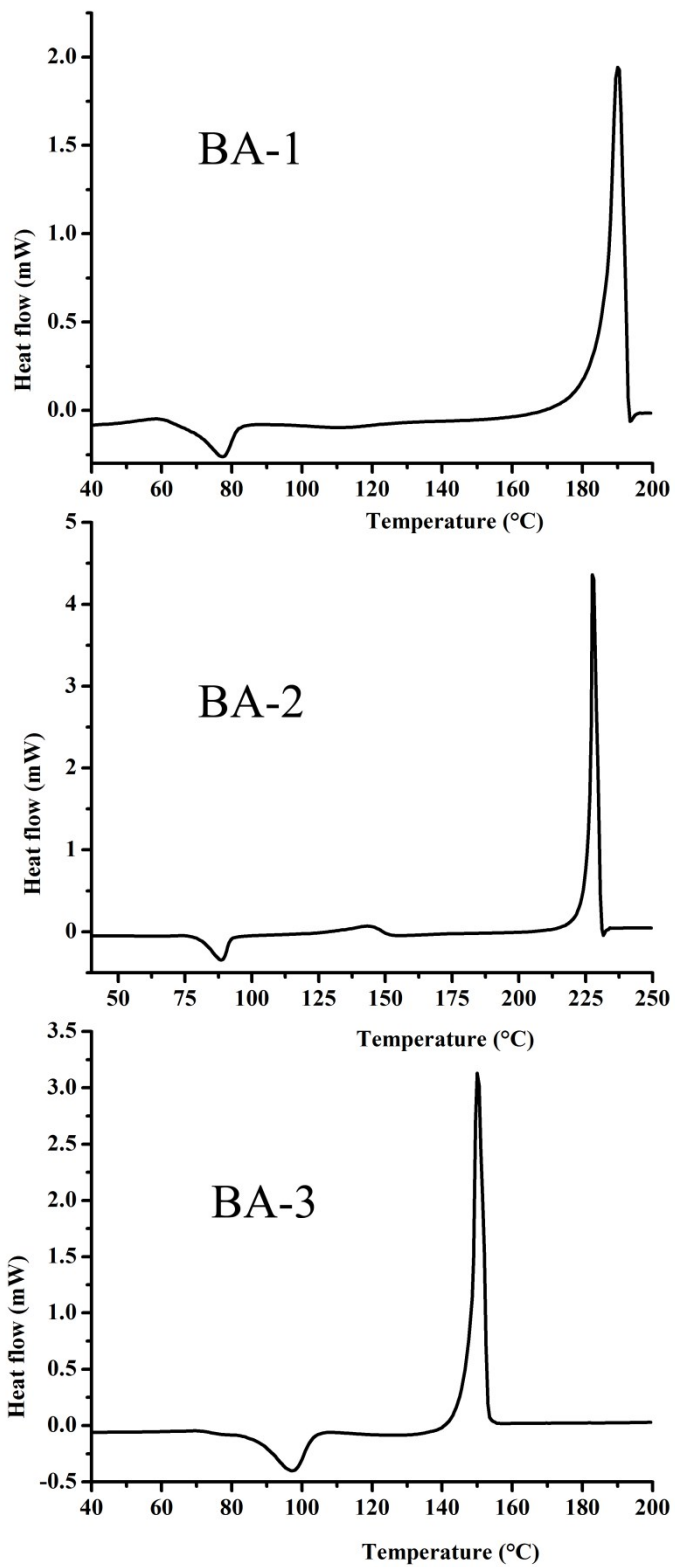


Fig. S13. DSC of BA-1-3.

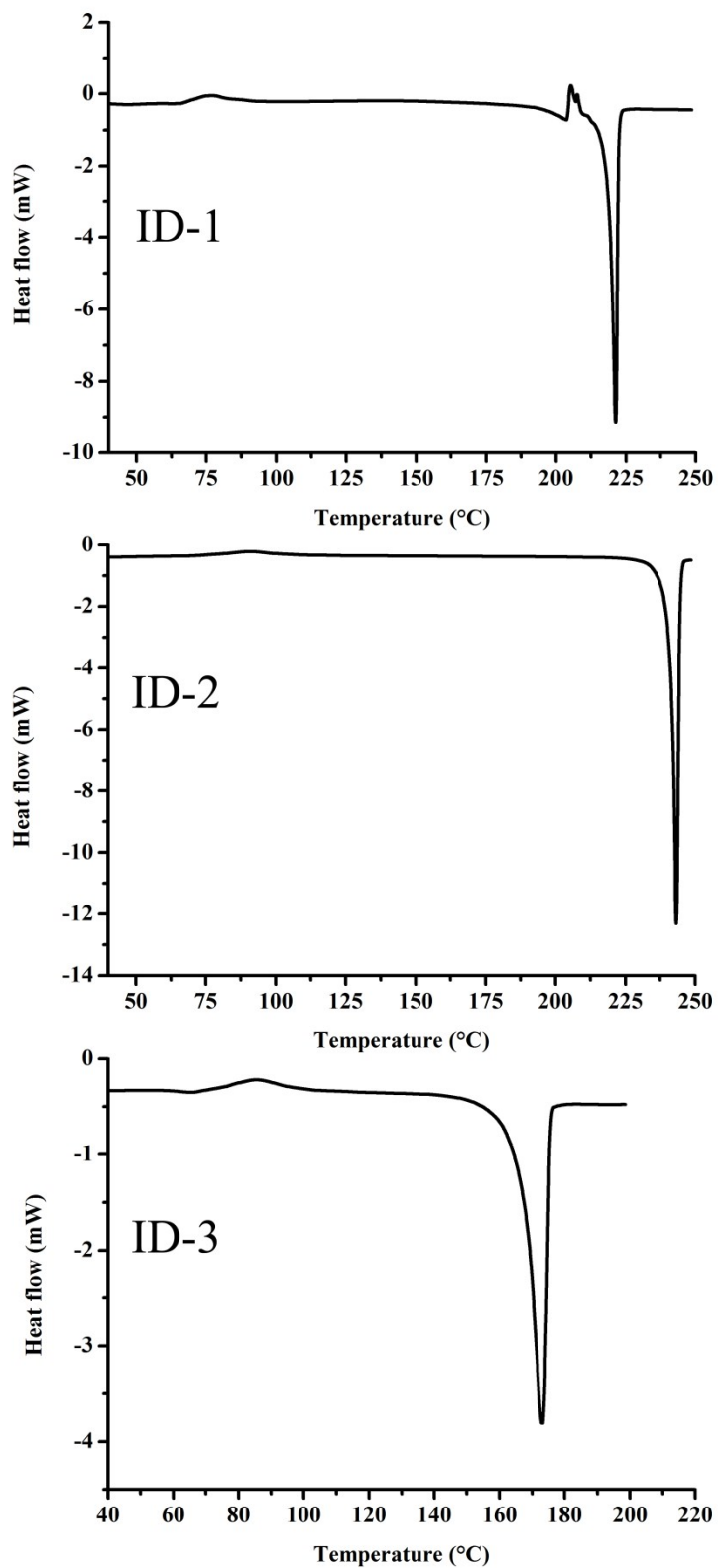


Fig. S14. DSC of ID-1-3.

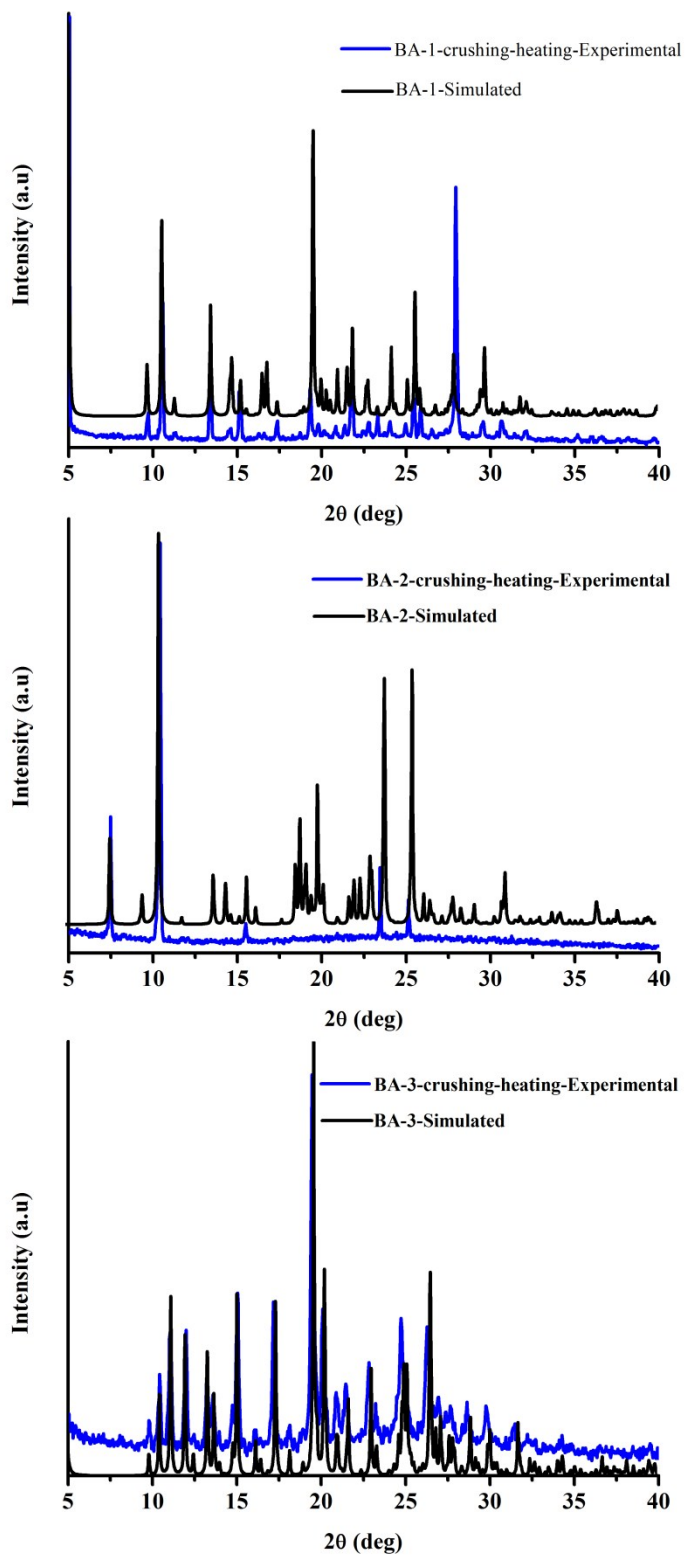


Fig. S15. PXRD pattern of (a) ID-2 and (b) ID-3 before, after hard crushing and heating.

